Sustainable Energy, Grids and Networks 35 (2023) 101120

Contents lists available at ScienceDirect

Sustainable Energy, Grids and Networks

journal homepage: www.elsevier.com/locate/segan

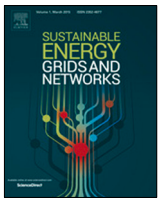

Smart electric vehicles charging with centralised vehicle-to-grid capability for net-load variance minimisation under increasing EV and PV penetration levels

M. Secchi [a,b,*], G. Barchi [a], D. Macii [b], D. Petri [b]

[a] Eurac Research, Institute for Renewable Energy, Viale Druso/Drususallee, 1, Bolzano/Bozen, 39100, Italy
[b] University of Trento, Department of Industrial Engineering, Via Sommarive 9, Trento, 38123, Italy

ARTICLE INFO

Article history:
Received 31 December 2022
Received in revised form 28 June 2023
Accepted 23 July 2023
Available online 26 July 2023

Keywords:
Electric vehicles (EV)
Smart EV charging
Photovoltaic Generator
Vehicle-to-grid

ABSTRACT

Increasing the share of Electric Vehicles (EVs) powered by renewable-based Distributed Energy Resources (DERs) is a key step towards climate neutrality. However, increasing the penetration of EVs and Photovoltaic (PV) generators may create large and hardly predictable fluctuations in power supply and demand, thus destabilising the grid. In this paper, an optimisation algorithm for smart EV charging is proposed to reduce the overall net-load variance through a more efficient exploitation of the available PV power, EV charging shifting, or vehicle-to-grid (V2G). Key distinctive features of the proposed approach are: (i) the formulation as a quadratic programming problem; (ii) the capability to enable a V2G charging policy, (iii) the inclusion of specific constraints regarding EVs' availability, owners' charging requirements and, partially, voltage stability; (iii) the study of the combined impact of EV and PV penetration on bus voltages, line currents, district self-sufficiency, and EV battery lifetime. The proposed approach is tested not only in ideal conditions, but also considering a basic persistence forecasting model of load and PV generation over subsequent days. The results of grid-level simulations in a case study show that the proposed approach could decrease the net-load variance by up to 60% if no forecasting errors occur and by about 50% when the persistence forecasting model is used. Additionally, the V2G policy notably decreases both the range of voltage fluctuations and the risk of line overloading, although at the expense of EVs' battery lifetime, whose reduction actually depends on the battery capacity.

1. Introduction

The European Union's (EU) aims at reducing greenhouse gases emissions by 55% compared to the levels recorded in 1990 [1]. For this purpose, it is essential to reduce the environmental impact of the mobility sector, which, per se, accounts for around 20% of the total worldwide carbon dioxide emissions in the atmosphere [2]. The conversion of a sizeable number of internal combustion engine vehicles (ICEVs) into fully electric vehicles (EVs) would definitely contribute to solve this problem [3,4], provided the electricity mix used to extract the necessary raw materials and charge their batteries is mainly based on renewable energy sources. However, the required number of both EVs and renewable sources, such as the photovoltaic (PV) systems, needs to grow in the next years. A large-scale deployment of EVs and PVs may pose a variety of business and technical challenges [5,6], especially at the distribution level, where large daily fluctuations of power demand and supply may jeopardise grid stability, which has to be constantly monitored, e.g., through fast and accurate state estimation techniques [7]. From a Distribution System Operator (DSO) perspective, the technical challenges are the most important ones, but their solution cannot be detrimental to the quality of service and the profitability expected by EV owners. Several studies found that the grid components which are likely to be most affected by the increasing penetration of EVs are the Medium-Voltage/Low-Voltage (MV/LV) transformers at the secondary substations (SS) [8,9]. Moreover, it is well-known that the time-varying charging of a large amount of EVs may cause voltage fluctuations [9–11], lines overloading [8,9,11], and/or power quality problems, such as frequency deviations [8,9,11], voltage imbalances [9,12,13], harmonics [14,15] and flicker [16,17]. As a consequence, it is difficult to comply with the requirements of local, national or international regulations, such as the EN Standard 50160:2010 [18]. The additional power demand peaks due to EVs could be mitigated through smart charging. This

* Corresponding author at: Eurac Research, Institute for Renewable Energy, Viale Druso/Drususallee, 1, Bolzano/Bozen, 39100, Italy.
E-mail addresses: mattia.secchi@eurac.edu (M. Secchi), grazia.barchi@eurac.edu (G. Barchi), david.macii@unitn.it (D. Macii), dario.petri@unitn.it (D. Petri).

https://doi.org/10.1016/j.segan.2023.101120

Nomenclature

ΔC^{CAL}	Capacity decrease due to calendar battery ageing.
ΔC^{CYC}	Capacity decrease due to cycling battery ageing.
δ	Range of allowable voltage fluctuation.
η	EV Charging/Discharging efficiency.
$\mathcal{B}''$	Subset of $\mathcal{B}'$ of the non zero-injection buses where at least one EV charging station is connected.
$\mathcal{B}'$	Subset of $\mathcal{B}$ collecting the non zero-injection buses only.
$\mathcal{B}$	Set of grid buses available on the grid.
$\mathcal{T}$	Set of the T time instants in a day.
$\mathcal{T}_s$	Subset of $\mathcal{T}$ collecting the instants of the sth charging session.
$\mathcal{U}$	Set of the M households connected to the network.
$\mathcal{U}_{EV}$	Subset of $\mathcal{U}$ including the N EV owners.
$\mathcal{U}_{PV}$	Subset of $\mathcal{U}$ including the K PV system owners.
σ_P	Variance of the active power flow at the transformer.
τ	Index of the charging instants in subset $\mathcal{T}_s$.
b	Index for a non zero-injection bus of the grid.
B'	Number of available non zero-injection buses on the grid.
C	EV battery capacity size.
EV_{share}	Share of the M households with an EV charging station.
I	Instantaneous battery current.
i	Index for the households.
I^{MIN}/I^{MAX}	Maximum and minimum allowable R.M.S. current values injected/absorbed into/from a nonzero-injection bus.
j	Index for the EV owners.
K	Number of households/users equipped with a PV system.
M	Number of households/users connected to the network.
N	Number of EV charging stations (and EVs).
NC^{EQ}	Equivalent number of full cycles performed by the EV battery during the year.
$NLVR$	Net Load Variance Reduction.
P^{Base}	Active power mismatch at the secondary substation transformer.
P^{Base}	Baseline power exchange at a nonzero-injection bus, when no EV charging stations are connected to the system.
p^{EV}	Instantaneous power absorbed by the EV charging station.
p^{LIM}	Maximum power absorbed by a user and measured by the domestic smart meter.
p^{LOAD}	Instantaneous power absorbed by domestic appliances.
P^{Net}	Instantaneous net power measured by the domestic smart meter.
p^{PV}	Instantaneous power produced by the PV system.
PV_{share}	Share of the M households with a PV system.
S	Number of daily sessions available for a specific EV.
s	Index for the EV charging session.
SC	Share of the PV production stored into the battery or directly consumed.
SOC^{end}	Minimum EV "departure" state-of-charge at the end of the charging session.
SOC^{init}	EV "arrival" state-of-charge at the beginning of the charging session.
SOC_{MAX}	Maximum attainable state-of-charge of the EV battery.
SOC_{MIN}	Minimum attainable state-of-charge of the EV battery.
SOH	State-of-health of the battery after 8 years of usage.
SP	Share of the household load covered by PV.
T	Number of time instants in a day (96).
t	Index for the simulation time instant.
T_K	EV battery pack temperature.
V^{Base}	Baseline voltage value at a nonzero-injection bus, when no EV charging stations are connected to the system.
V_0	Nominal grid voltage (r.m.s. value).
y	Year of EV usage, counting from purchase day.

can be achieved by using a variety of scheduling algorithms to modulate the amount of power drained from the grid, not only depending on the actual urgency of charging the battery, but also to support the grid [19–21]. Indeed, modern power electronics converters allow EVs to either absorb or inject electrical power in the grid if suitable *bidirectional* vehicle-to-grid (V2G) control schemes are implemented. In this regard, the distinction between a "centralised" V2G algorithm (where the charging is entirely demanded to a central control unit) and a "decentralised" V2G scheme (where EV owners can decide whether to charge the battery or not at predefined time slots) is crucial. Usually, the active power support to shave the power demand peaks at the transformer is more effective if all the EV charging stations are able to cooperate. Therefore, in this case, a *centralised* V2G scheme (in which EV charging or discharging is entirely managed by an aggregator) is preferable, especially when a large fleet of EVs is considered. The problem of centralised V2G control becomes even more important if not only the EV load profiles, but also the power generation ones change as a function of time, e.g., as a result of the increasing PV penetration.

In this paper, an automated strategy for EV charging with V2G capability is proposed and analysed in-depth, considering the EV-PV interaction as well. The proposed approach aims at minimising the overall net-load variance (NLV), and consequently the bus voltage variability, on an existing distribution grid. The baseline

load and PV penetration levels are given as input profiles, and smart EV charging is leveraged only.

The main elements of novelty presented in this work are summarised below:

- Even if initially we assume perfect knowledge of both load profiles and EV availability for active power support, the effect of possible deviations between the expected scenario and the real one in subsequent days is evaluated through a basic persistence forecasting model of load and PV generation profiles, showcasing the good robustness of the proposed approach in realistic conditions.
- The interaction between EVs and PV systems is analysed in a broad set of scenarios, ranging from the present low penetration levels of PVs and EVs to future scenarios when PV and EV penetrations are instead supposed to be much stronger.
- A repeated power flow analysis with a 15-minute time step is performed to assess to what extent the proposed centralised V2G-based optimisation strategy is beneficial in terms of voltage stability.
- Finally, a preliminary study on battery wear (one of the most debated aspects of V2G-based charging policies) is presented.

The rest of the paper is structured as follows. In Section 2, the specific contribution of this paper in the context of the related work is briefly presented. In Section 3, the optimisation problem and the underlying methodology are formalised. Section 4 describes the key features of a relevant case study along with the main simulation settings. Section 5 reports a quantitative performance evaluation of the proposed optimal smart EV charging approach. Finally, Section 6 provides an overview of the broader impact of the proposed technique on: users' energy requirements for self-sufficiency, grid voltage stability and EV battery wear. Finally, Section 7 concludes the paper.

2. Related work

Some of the most significant methodologies proposed in the literature to perform smart EV battery charging (possibly empowered by V2G) are listed in Table 1. Due to the broad variety of possible objective functions, we classified the relevant literature based on the objective functions: (1) minimising peak load demand (peak-shaving/valley-filling); (2) maximising the exploitation of distributed energy resources (DERs); (3) any methodologies combining different objectives (such solutions are labelled as "hybrid" in Table 1); (4) balancing the grid net-load; (5) minimising the grid Net-Load Variance (NLV).

The papers included in the first group present methodologies aimed at peak-shaving and valley-filling the active grid load profiles, at both the substation and the single-building levels. In [22], for example, a constraint-scheduling programming approach was used, whereas in [23] non-linear programming was chosen. Some other authors instead preferred a variety of meta-heuristic algorithms [24–28] to centrally schedule EV charging. Rule-based controls were also used in [29–35] to solve the EV scheduling problem in a centralised and decentralised way, respectively. In all these papers, the presence of DERs is not considered, but in the near future, as the DER penetration increases, this aspect will become fundamental. In this paper, peak-shaving is performed as the NLV is mitigated.

In the second group of papers, EVs batteries are generally charged with a surplus of DERs, usually with the aim to reduce the cost of electricity from wind or PV generators, and/or to minimise grid-related emissions. Among those papers, in [36], a deep learning algorithm is used to maximise the usage of the PV production, whereas in [19] mixed-quadratic programming is applied to avoid PV curtailment. In [37], the same approach is chosen and improved through game theory. A combination of particle swarm optimisation and a rule-based control is instead used in [38] to perform decentralised smart EV charging. Maximising the use of DERs is a fundamental step for the implementation of clean power systems, but it is just half of the problem. Indeed, extreme peak consumption levels at the substation should be limited level as well, in order to avoid grid congestion and undervoltage issues. This aspect is considered when minimising the NLV, the objective function we chose for this work.

A variety of tasks can be accomplished by pairing the aforementioned objectives to additional ones, such as performed in the works from the third group. For example, NLV minimisation could be paired to system costs minimisation [46,53], wind power fluctuations reduction [39], or power losses and transformer tap switching minimisation [47]. In [20,45,54,55] for instance net-load minimisation is paired to EV charging costs minimisation, whereas in [43] voltage regulation is performed, and in [44] the charging session temperature and duration are minimised. Peak shaving is paired with EV charging costs minimisation in [40–42], but EV grid services revenue is also targeted in [48,49,51]. Finally, in [42,50] the grid impact is minimised, while the Authors of [50,52] try to limit the impact of smart charging on the usability of the EVs. These algorithms, are capable of simultaneously minimising/maximising multiple, often contrasting, objectives, but they cannot fully assess the capability of EV smart charging to smooth the aggregated active power profile to support PV generation. More in detail, meta-heuristics are powerful tools to speed-up the search for the optimal solution, but can get stuck in local minima and are generally preferred when it is not possible to represent the optimisation function mathematically, as it happens in this work for the NLV.

Authors from the last two groups of papers try to minimise the fluctuations of the grid net-load instead, either by not choosing or choosing the net-load variance as the objective function. In group four, linear programming is compared to a rule-based algorithm for decentralised EV smart charging [56], whereas mixed integer programming and non-linear programming are sometimes chosen, as in [57,59], respectively. Rule-based controls were also applied in [61,62] (centralised) and [60] (decentralised), whereas forecasting was added in a model predictive control algorithm [58]. Authors in group five instead, explicitly choose to minimise the NLV through centralised rule-based controls [68–70]. Model-predictive control is deployed in [63] instead. Some other Authors use quadratic [10,66,67] or sequential quadratic [71,72] programming method instead, since NLV is inherently a quadratic function. Rule-based and model-predictive controls, although very effective and easy-to-implement in the real world, can hardly be used to investigate the potential benefits of centralised V2G-based policies over a time horizon of several hours or days, since they typically optimise the EV charging schedule at every time step relying on the present data only. Conversely, the smart EV charging solutions leveraging mathematical "programming" techniques over long time intervals are difficult to apply in practice, because they require a forecasting of the users' activities. Indeed, the actual schedule of such activities may notably differ from the expected one. The methodology presented in this paper lies in between the two aforementioned extreme visions, since it does not address a real-time optimal scheduling problem, but at the same time it provides a solution that, with a reasonable lag, can be used to define a realistic EV charging schedule. In fact, the information collected during a full day is used to find the optimal EV charging schedule minimising the NLV, while including realistic constraints on EVs usage. Such a

Table 1
Relevant literature overview on smart EV charging techniques with a focus on active power support.

Objective	Methodology	Type	Examples
(1) Peak-Shaving+Valley-Filling	Constraint Scheduling Programming	Centralised	[22]
	Non-Linear Programming	Centralised	[23]
	Meta-Heuristics	Centralised	[24–28]
	Rule-Based Control	Centralised	[29–31]
	Rule-Based Control	Decentralised	[32–35]
(2) Maximising DER Utilisation	Deep Reinforcement Learning	Centralised	[36]
	Mixed-Integer Quadratic Programming + Game Theory	Decentralised	[37]
	PSO + Rule-Based Control	Decentralised	[38]
	Mixed-Integer Quadratic Programming	Centralised	[19]
(3) Hybrid	Alternating Direction Method of Multipliers	Decentralised	[39,40]
	Deep Learning	Centralised	[41,42]
	Edge Computing+Rule-Based Control	Centralised	[43]
	Meta-Heuristics	Decentralised	[44–48]
	Mixed-Integer Linear Programming	Centralised	[49]
	Model Predictive Control	Centralised	[50]
	Quadratic Programming	Centralised	[20]
	Rule-Based Control	Centralised	[51–53]
	Stochastic Dynamic Programming	Decentralised	[54]
	Fuzzy Control	Decentralised	[55]
(4) Net-Load Balancing	Linear Programming or Rule-Based Control	Decentralised	[56]
	Mixed-Integer Linear Programming	Centralised	[57]
	Model Predictive Control	Centralised	[58]
	Non-Linear Programming	Centralised	[59]
	Rule-Based Control	Decentralised	[60]
	Rule-Based Control	Centralised	[61,62]
(5) Minimising NLV	Model-Predictive Control	Centralised	[63]
	Meta-Heuristics	Centralised	[64,65]
	Quadratic Programming	Both	[66]
	Quadratic Programming	Decentralised	[10,67]
	Rule-Based Control	Centralised	[68–70]
	Sequential Quadratic Programming	Centralised	[71,72]

global solution is found by solving a quadratic programming (QP) problem, and it is eventually used to define the EV charging schedule of the following day (i.e., assuming a basic persistence model). Even if the actual NLV reduction is lower than in ideal conditions, the results are still rather good, as it will be clearly shown in Section 5.

Moreover, the analysis of the impact of smart EV charging on a LV distribution grid and the EVs battery degradation are further novelties of this paper. In fact, only in [10,19,43,66,72], the Authors perform a proper power-flow analysis to assess the combined impact of PV and EV systems on bus voltage stability and line loading, but none of them investigates the effects on battery degradation, which is only considered in [24,51]. Thus, to the best of our knowledge, our work is the only one considering all these aspects at the same time.

3. Problem formulation

Let us consider an LV distribution system consisting of a set $\mathcal{B}$ of B buses and a set $\mathcal{U}$ of M users. If $\mathcal{U}_{PV}$ and $\mathcal{U}_{EV}$ are the subsets of $\mathcal{U}$ including the $K \leq M$ and the $N \leq M$ users equipped with a PV system or an EV charging station, respectively, then we can denote with $PV_{share} = \frac{K}{M}$ and $EV_{share} = \frac{N}{M}$ the corresponding shares of users. Assuming, for the sake of simplicity, but without loss of generality, that

- each user owns at most one EV;
- no energy storage systems different from the EV batteries are deployed in the grid;
- the actual amount of power consumed and generated by each user is supposed to be monitored by a centralised aggregator, as customary in centralised smart EV charging schemes [19,20]. However, only the EV charging stations are actually controlled to schedule V2G-based battery smart charging.
- each EV is connected to a single proprietary charging station;

the average net power absorbed from or injected into the grid by the ith user within the tth metering time slot of duration Δt is

$$p_{i,t}^{Net} = p_{i,t}^{LOAD} + p_{i,t}^{EV} - p_{i,t}^{PV}, \quad i \in \mathcal{U} \quad t \in \mathcal{T} \tag{1}$$

where $\mathcal{T} = \{1, \ldots, T\}$ is set of T time slots in a given time interval (e.g., one day), $p_{i,t}^{LOAD}$ is the user's average load consumption for house appliances within the tth time slot, and $p_{i,t}^{EV}$, $p_{i,t}^{PV}$ (which are different from 0 only if $i \in \mathcal{U}_{EV}$ and/or $i \in \mathcal{U}_{PV}$) are the additional average EV power consumption and the generated average PV power, respectively, in the same time slot t.

Quite importantly, the sequences of $p_{i,t}^{LOAD}$ and $p_{i,t}^{PV}$ values (if user i actually owns a PV system) can be regarded as inputs to the proposed optimisation problem, as they depend on the actual solar irradiation as well as on the PV capacity installed by each user. On the contrary, all terms $p_{i,t}^{EV}$ can be regarded as the decision variables of the optimisation problem, as they can

be actually modified by the adopted smart EV charging policy (if any). As a consequence, the values of $p^{EV}_{i,t}$ are positive when the EV is connected to the charging station and the battery is under charge, while they become negative if a V2G policy is adopted for reverse power flow mitigation.

In practice, the M users are connected to a subset $\mathcal{B}' \subseteq \mathcal{B}$ of the available grid buses. Usually, $B' = |\mathcal{B}'|$ is strictly lower than B because of the zero-injection buses commonly present in distribution systems. If sets $\mathcal{U}^b$, $\mathcal{U}^b_{PV}$ and $\mathcal{U}^b_{EV}$ for $b = 1, \ldots, B'$ are the sets resulting from the partition of $\mathcal{U}$, $\mathcal{U}_{PV}$ and $\mathcal{U}_{EV}$ depending on how the M users are connected to the available buses, then it follows from (1) that the aggregate net load at bus $b \in \mathcal{B}'$ in the tth metering time slot is

$$P^{Net}_{b,t} = \sum_{i \in \mathcal{U}^b} p^{Net}_{i,t} = P^{Base}_{b,t} + \sum_{i \in \mathcal{U}^b_{EV}} p^{EV}_{i,t}, \quad b \in \mathcal{B}' \quad t \in \mathcal{T} \tag{2}$$

where the sequence of values $P^{Base}_{b,t} = \sum_{i \in \mathcal{U}^b} p^{LOAD}_{i,t} - \sum_{i \in \mathcal{U}^b_{PV}} p^{PV}_{i,t}$ for $t \in \mathcal{T}$ is the net load of the bth bus when no EVs are considered. If the net load values per bus given by (2) are summed up, then the overall aggregate net load over the grid within the $t-$th time slot is

$$P^{Net}_{t} = \sum_{b \in \mathcal{B}} P^{Net}_{b,t} = P^{Base}_{t} + \sum_{i \in \mathcal{U}_{EV}} p^{EV}_{i,t}, \quad t \in \mathcal{T} \tag{3}$$

where the sequence of values $P^{Base}_{t} = \sum_{b \in \mathcal{B}} P^{Base}_{b,t}$ for $t \in \mathcal{T}$ is the baseline net load profile whose peaks should be smoothed through smart EV charging.

If we denote with $i_1, \ldots, i_N$ the indexes of the users in the subset $\mathcal{U}_{EV} \subseteq \mathcal{U}$, the vector of decision variables in the rightmost side of (3) can be rearranged into a single $T \cdot (N+1)-$long column vector regardless of the bus where different users are connected, i.e.,

$$\mathbf{P} = [P^{Base}_1, p^{EV}_{i_1,1}, \ldots, p^{EV}_{i_N,1}, \ldots, P^{Base}_T, p^{EV}_{i_1,T}, \ldots, p^{EV}_{i_N,T}]^T. \tag{4}$$

Thus, through a few basic algebraic steps it can be shown that the maximum likelihood estimator of the daily aggregated NLV can be rearranged into a matrix form as follows, i.e.,

$$\sigma^2_P(\mathbf{P}) = \frac{1}{T} \cdot \sum_{t=1}^{T} \left(P^{Net}_t - \frac{1}{T} \sum_{t=1}^{T} P^{Net}_t \right)^2 = \frac{1}{2} \mathbf{P}^T \mathbf{H} \mathbf{P} \tag{5}$$

where

$$\mathbf{H} = \frac{2}{T^2} \begin{bmatrix} (T-1)\mathbf{U}_{N+1} & -\mathbf{U}_{N+1} & \ldots & -\mathbf{U}_{N+1} \\ \vdots & \vdots & \ddots & \vdots \\ -\mathbf{U}_{N+1} & -\mathbf{U}_{N+1} & \ldots & (T-1)\mathbf{U}_{N+1} \end{bmatrix} \Bigg\} \text{T blocks}$$

is a square matrix composed by $T \times T$ blocks including the $(N+1) \times (N+1)$ all-ones matrix $\mathbf{U}_{N+1}$, multiplied by either $T-1$ or -1.

Given that (4) is the vector of the decision variables used to schedule the battery charging of all EVs over the considered time interval and (5) is the chosen objective function, the corresponding optimisation problem can be easily formalised as follows, i.e.,

$$\min_{\mathbf{P}} \ \sigma^2_P(\mathbf{P}). \tag{6}$$

Expression (5) confirms that the chosen objective function can be rearranged into a quadratic form. If such a function is convex, a QP solver can converge to the solution of (6) within a polynomial time. To this end, standard QP solving tools can be used, as explained at the beginning of Section 5. Of course, in order to find a correct and realistic EV charging schedule, a number of further constraints must be included. Such constraints are explained and formalised below.

1. **Constraints due to baseline net-load conditions**. The elements P^{Base}_t of (4) have to be excluded from the optimisation process, since, as explained above, the aggregate base net-load values are in fact just an input to the optimisation problem. Thus, the following equality constraints must be applied, i.e.,

$$P^{Base}_t = P^*_t, \quad t \in \mathcal{T} \tag{7}$$

where P^*_t for $t = 1, \ldots, T$ is the overall net power demand profile (excluding the EVs) measured at the transformer in each time slot.

2. **Constraints on EV battery charging**. In every metering time slot t, each EV can be either connected to or disconnected from its own charging station, depending on actual users' needs. Assuming that S_j (for $j = 1, \ldots, N$) is the number of the daily charging sessions of the EV of user $i_j \in \mathcal{U}_{EV}$, and denoting with $\mathcal{T}_{s,j} \subseteq \mathcal{T}$ the subset of time slots of the sth charging session of vehicle of user i_j (i.e., for $s = 1, \ldots, S_j$), the following equality constraints on EVs' battery state-of-charge (SOC) must be met to ensure that each EV battery is charged enough according to users' expectations, i.e.,

$$\sum_{t \in \mathcal{T}_{s,j}} \frac{\eta_j}{C_j} p^{EV}_{i_j,t} \Delta t = (SOC^{end}_{s,j} - SOC^{init}_{s,j}) \qquad s = 1, \ldots, S_j, \quad j = 1, \ldots, N \tag{8}$$

In (8) constants η_j and C_j represent the battery charging efficiency and the battery capacity of the EV of user i_j, while $SOC^{init}_{s,j}$ and $SOC^{end}_{s,j}$ are the battery SOC values at the beginning and at the end of the sth charging session, respectively. It is important to emphasise that both $SOC^{init}_{s,j}$ and $SOC^{end}_{s,j}$ are just inputs to the optimisation problem, as they depend on the actual use of the jth EV. The $SOC^{init}_{s,j}$ values can be measured as soon as the EV is connected to the charging station, while the $SOC^{end}_{s,j}$ values are usually close to the maximum attainable SOC.
Besides (8), a further set of inequality constraints must be applied during each EV charging session to prevent excessive battery charging or discharging (in V2G mode) i.e.,

$$SOC_{MIN} \leq SOC^{init}_{s,j} + \sum_{t \in \mathcal{T}_{s,j}}^{\tau} \frac{\eta_j}{C_j} p^{EV}_{i_j,t} \Delta t \leq SOC_{MAX} \qquad \forall \tau \in \mathcal{T}_{s,j} \ \ s = 1, \ldots, S_j, \ \ j = 1, \ldots, N. \tag{9}$$

The sum is verified for each time instant $\tau \in \mathcal{T}_{s,j}$, so that the limit is respected for each charging session instant. This is needed to prevent faster battery wear, as highlighted in [73,74]. Note that, even if the lower and upper threshold values SOC_{MIN} and SOC_{MAX} actually depend on battery type, size, and manufacturer, these limits will be assumed to be the same for all vehicles for the sake of simplicity.

3. **Constraints due to EVs unavailability**. When an EV is not connected to the charging station, of course its battery can neither be charged, nor it can be used for V2G-based active power support. Therefore, the following equality constraints have to be applied, i.e.,

$$p^{EV}_{i_j,t} = 0 \quad t \in \mathcal{T}_{d,j}, \quad i_j \in \mathcal{U}_{EV} \tag{10}$$

where $\mathcal{T}_{d,j} = \mathcal{T} \backslash (\bigcup_{s \in S_j} \mathcal{T}_{s,j})$ includes all time slots when the EV of user i_j is not connected to any charging station and the battery is discharged during a driving session.

4. **Constraints on maximum EV charging and discharging power**. Due to contractual restrictions, technology limitations and/or safety reasons, the EV charging and discharging power cannot exceed a given limit $\pm P_j^{LIM}$. Therefore, a further set of inequality constraints to apply when solving the optimisation problem is given by

$$|p_{i_j,t}^{EV}| \leq P_j^{LIM} \quad t \in \mathcal{T} \;\; i_j \in \mathcal{U}_{EV}. \tag{11}$$

In the rest of this paper, for the sake of simplicity but with no loss of generality, we will assume that the charging/discharging power limits are the same for all charging stations, i.e., $P_j^{LIM} = P^{LIM}$, for $j = 1, \ldots, N$.

5. **Constraints due to grid voltage limits**. Even if any smart EV charging technique is inherently supposed to shave the baseline net load power peaks (thus mitigating the voltage fluctuations as well), a final set of constraints should be included in the optimisation problem to ensure that the upper and lower voltage limits are not violated at the buses where the power injections can be partly controlled through the decision variables of the problem, namely the EV charging/discharging power values. In particular, if $\mathcal{B}'' \subseteq \mathcal{B}' \subseteq \mathcal{B}$ is the subset of the non-zero-injection buses whose power injection depends on at least one EV charging station, then the following set of further grid-related constraints can be added to the problem, i.e.,

$$V_0(1-\delta)|I_{b,t}^{MAX}| \leq \left| P_{b,t}^{Base} + \sum_{i_j \in \mathcal{U}_{EV}^b} p_{i_j,t}^{EV} \right| \leq V_0(1+\delta)|I_{b,t}^{MIN}|$$
$$t \in \mathcal{T}, \quad b \in \mathcal{B}'' \tag{12}$$

where V_0 is the root mean square (RMS) value of the nominal grid voltage, $\pm\delta$ is the maximum relative range of voltage values compliant with the adopted regulation (e.g., the EN Standard 50160:2010, as explained more in detail in Section 4.5 [18]), and $|I_{b,t}^{MIN}|$, $|I_{b,t}^{MAX}|$ are the absolute values of the minimum and maximum possible RMS current injections at bus b within time slot t. The absolute value operator is needed in (12) to address the case of possible reverse power flows whenever the amount of generated PV power exceeds the local power demand. The sequence of values $I_{b,t}^{MIN} = \frac{P_{b,t}^{Base}}{V_{b,t}^{Base}}$ (where $V_{b,t}^{Base}$ is the voltage values at bus b in time slot t) results from the repeated power flow analysis in the baseline case, i.e., when the consumption due to EVs is negligible. The dual sequence $I_{b,t}^{MAX}$ results instead from the power flow analysis of the grid when all the charging stations connected to bus b charge the EVs actually available in a given time slot at the maximum rate, i.e., P^{LIM}, as it commonly happens when no smart EV charging strategies are used. Both power flow analyses for a given EV and PV penetration levels can be run before running the optimisation algorithm itself, allowing for the calculation of the parameters from (12).

It can be observed that constraints (7)–(12) are all linear and can be easily formalised in a matrix form by using sparse matrices. Therefore, they are simple to implement and the memory requirements are reasonable.

4. Case study description

This Section describes the features of the LV distribution grid used as a case study, the baseline load profiles, and the way in which both the EV usage profiles and the PV generation patterns are generated. A summary of the general simulation settings and scenarios that were considered to evaluate the performance of the proposed V2G-based EV smart charging strategy is also presented in the following.

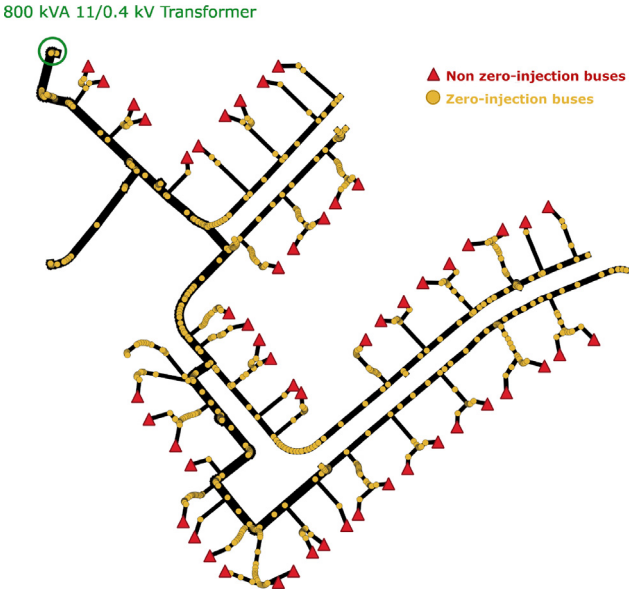

Fig. 1. IEEE 906 bus LV map[1]. Line thickness is proportional to lines ampacity, whereas the non zero-injection buses are highlighted with red markers. (For interpretation of the references to color in this figure legend, the reader is referred to the web version of this article.)

4.1. Grid model

The distribution system used as a case study is the IEEE 906-bus LV Test Feeder[1], which is an example of a typical 240 V European LV grid, with a 800 kV A transformer, lines' ampacities ranging between 200 and 500 A for the main lines, and between 50 and 80 A for the secondary ones [75]. Fig. 1 shows a simplified map of the distribution system used as a case study.

4.2. Baseline load profiles

The daily power consumption profiles of $M = 297$ households were synthesised through LPG,[2] a bottom-up software application that mimics the domestic electricity demand of different kinds of users depending on their daily activities. The baseline power demand profiles consider the buildings stock composition and the dwellers' age distribution of the city of Bolzano/Bozen, Italy, according to ASTAT[3] data. The buildings stock consists of single-family (i.e., detached) houses and buildings with four or six flats. The contractual power demand of each household is assumed to be 4.5 kW (although 3 kW is currently the most common scenario in Italy for residential users) in order to safely accommodate the additional load due to EV charging (see Section 4.4). The median values and the range of variation (between the 25th and the 75th percentiles) of the weekly baseline load profiles per user in summer and winter, respectively, are shown (in blue) in Fig. 2. The corresponding overall monthly energy consumption for the summer scenario lies between 93 kW h and 356 kW h, whereas in winter it ranges between 121 kW h and 388 kW h. The power factor values were randomly chosen between 0.95 and 1.

[1] IEEE LV Test Feeder: https://site.ieee.org/pes-testfeeders/

[2] LPG: A Bottom-Up Customizable Load Generator, Noah Pflugradt, https://www.loadprofilegenerator.de

[3] ASTAT: Statistics Institute for the Autonomous Province of South-Tyrol

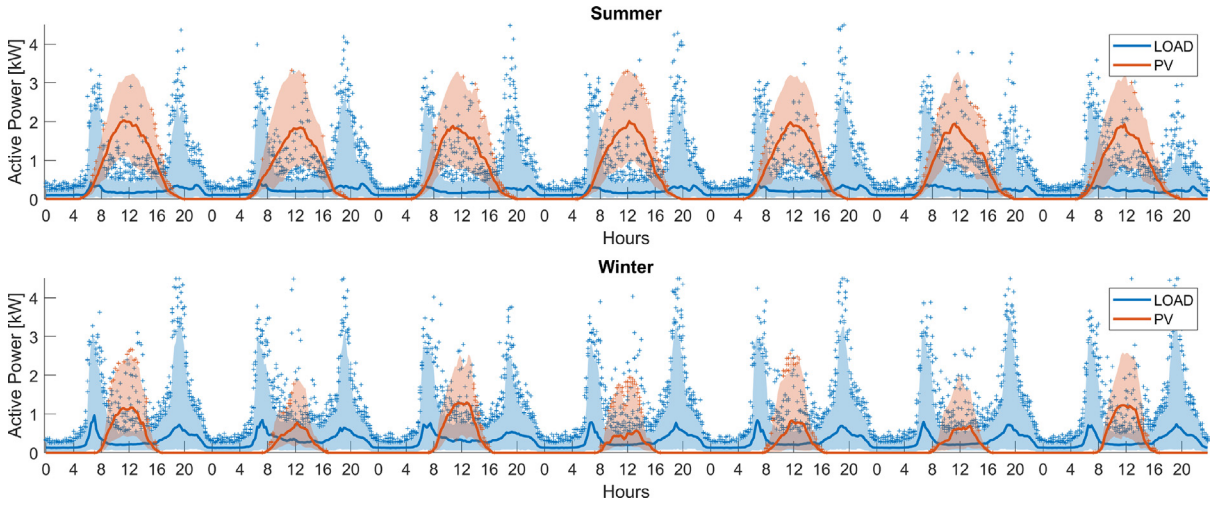

Fig. 2. Median values (thick lines) and range of variation between the 25th and the 75th percentiles (shaded areas) of the weekly baseline load profiles (in blue) and the corresponding weekly PV generation profiles (in red) per user in summer and winter, respectively. (For interpretation of the references to color in this figure legend, the reader is referred to the web version of this article.)

4.3. PV generation profiles

Due to the limited geographical area of the considered LV distribution grid and for the sake of simplicity, all users are assumed to share the same irradiation and panel temperature profiles. In the considered case study, such data are experimental, as they were collected at the airport of Bolzano/Bozen (Italy) every 15 min in 2019. The variation in the weekly PV generation profiles per user are shown (in red) in Fig. 2. The PV systems were connected the same phases as the user appliances loads they serve, assuming they are used primarily for self-consumption. Of course, the installed PV capacity (if any) differs from user to user. In particular, the size of PV systems is computed in such a way that the amount of energy typically produced over one year and the corresponding yearly energy consumption approximately coincide [76]. As a consequence, the resulting installed PV capacities per household generally range between 1.5 kW and 4 kW, in steps of 250 W, in accordance with [76]. The use of PV modules of greater size (450 W) changes the resolution of the PV profiles, but do not affect the results of the present study, because the proposed smart EV charging algorithm depends on aggregated quantities and not on the size of individual PV modules. The monthly PV energy ranges between 220 kW h and 586 kW h in summer, and between 74 kW h and 198 kW h in winter, with a maximum instantaneous generation of 3.5 kW in summer and 2.6 kW in winter.

4.4. EV load profiles

The EV consumption and constant-current charging profiles based on EVs' supposed usage were generated with the RAMP-mobility[4] software tool [77], by setting the shares of plug-in hybrid EVs (PHEVs), battery EVs (BEV) and their battery capacity. The shares of PHEV and BEVs are assumed to be 60% and 40%, respectively,[5] while the battery capacity is around 8–10 kW h for PHEVs and between 30 and 100 kW h for BEVs.[6] Assuming to deploy LV, single-phase 16-A charging stations compliant with the IEC Standard 61851-1:2010 [78], the maximum EV charging and discharging power P^{LIM} was set to 3.7 kW, which is below the chosen contracted capacity of every single user and it is in line with the values used in other research works [10,79]. The EV charging–discharging efficiency η in (8)–(9) is around 0.9, as in [10,80]. The monthly EV energy consumption per user ranges between 170 kW h and 239 kW h, totalling 1.6–3.2 MW h/year. The resulting average yearly EV energy consumption is in good agreement with the Italian car driving surveys [81], assuming that each EV travels 31 km per day on average, and its consumption is around 0.23 kW h/km. In the rest of this paper, the baseline simulations when no smart EV charging is used rely on the assumption that each EV connected to a charging station can drain the maximum allowed amount of power until the target SOC is reached.

4.5. Simulated scenarios

The main simulation settings in different scenarios are briefly summarised below:

- The adopted IEEE LV grid is described just by a three-phase model with $B' = 56$ non-zero-injection buses, while the $M = 297$ load profiles refer to single-phase users. Therefore, for simulation purposes, the users' load profiles must be aggregated and they can be assigned to the different phases of the non-zero-injection buses of the LV test distribution system in such a way that the system is reasonably balanced. Since all profiles change over time, we cannot rule out the possibility of some imbalance, which is normal in standard operating conditions. However, since the users' power profiles exhibit a similar shape, if the same number of users is connected to each phase of a given bus, the risk of severe voltage imbalances is rather low. The total aggregated power profiles were used to compute the baseline values P_t^* in (7).
- The simulation time step is set to 15 min, which provides a good trade-off between computational complexity and simulation accuracy [82]. This is quite realistic because some last-generation smart meters (including those recently deployed in Italy) can measure and transmit the power/energy consumption values every 15 min. As a result, considering a daily forecasting, we have that $T = 96$ steps.

[4] RAMP-mobility: a RAMP application for generating bottom-up stochastic electric vehicles load profile https://github.com/RAMP-project/RAMP-mobility

[5] Motus-E Market Analysis for Italy, https://www.motus-e.org/analisi-di-mercato/gennaio-2022-i-primi-segnali-dellassenza-di-incentivi

[6] EV Database Org, https://ev-database.org/cheatsheet/useable-battery-capacity-electric-car

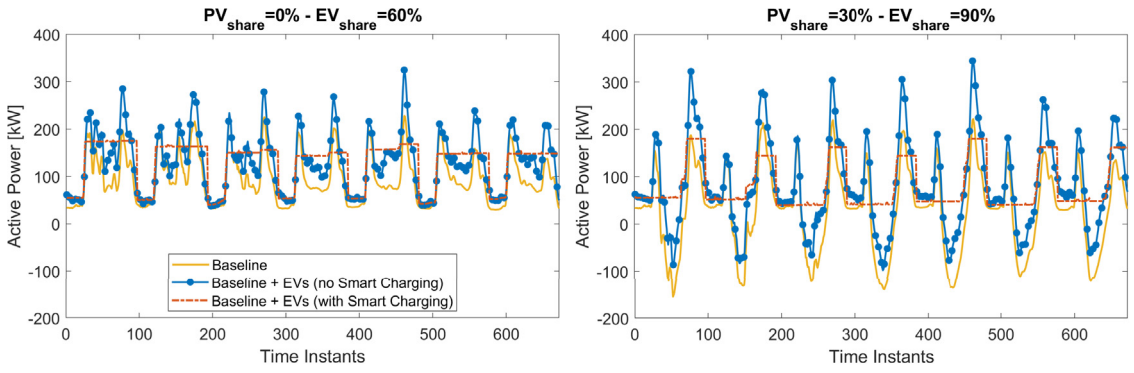

(a) Summer scenario

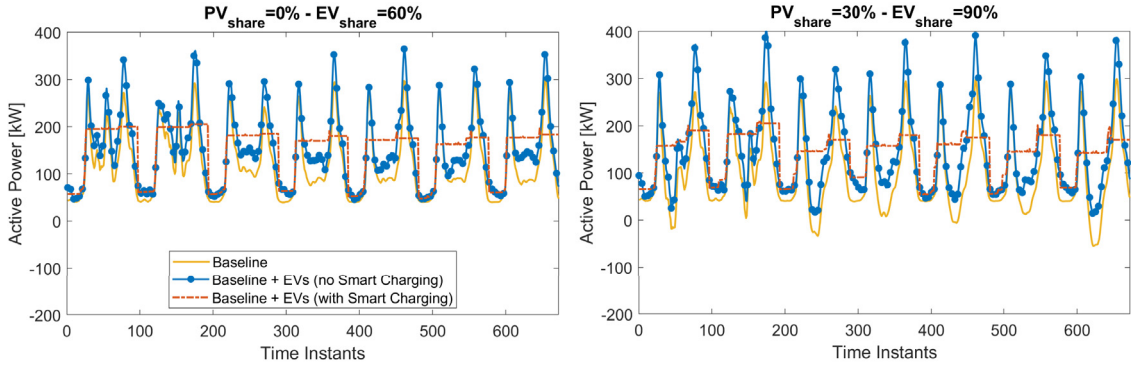

(b) Winter scenario

Fig. 3. Active net-load power profiles at the substation transformer without EVs and with 60% of users provided with EVs both without and with adopting the proposed V2G-based smart charging policy. The plots in (a) and (b) refer to the summer and winter scenarios, respectively, assuming that the shares of users equipped with PV systems are 0% (left) or 30% (right).

- To explore the joint impact of different levels of EV and PV penetration, the values of parameters EV_{share} and PV_{share} are increased from 10% to 90% and from 0% to 90%, respectively. In all cases, the users equipped with a PV system and/or with an EV charging station are selected randomly, and assigned to the three-phases of the distribution systems in such a way that the system is reasonably balanced. Of course, the number of buses within set $\mathcal{B}''$, as well as the number of both decision variables and constraints depend on the chosen EV_{share} value.
- The values of the relative voltage limits δ used in constraint (12) are set in compliance with the requirements of the EN Standard 50160:2010 [18], prescribing that the 10-minute mean r.m.s. values of the supply voltage shall be within the $\pm 10\%$ range for 95% of the measured samples.

To keep the overall computation time within reasonable limits, the optimal EV charging schedules for each pair of EV_{share} and PV_{share} values were computed day-by-day over an average week in summer and winter, respectively, namely when the solar irradiation is close to its maximum and its minimum, respectively.

5. Optimisation results

The smart EV charging algorithm was implemented in Matlab, and it relies on the standard *quadprog* function of the Optimization Toolbox to solve the core QP problem. All data structures were built and formatted to make them compatible with *quadprog*, possibly using the *sparse* operators to reduce the memory requirements whenever possible. Figs. 3(a)–3(b) shows the aggregated weekly net-load profiles at the substation transformer computed both without considering the EVs and with the additional loads due to EV charging when $EV_{share} = 60\%$. In the latter case, both the profiles obtained with constant EV charging (lines with circle markers) and those resulting from the proposed V2G-based smart charging policy (dashed lines) are plotted. Figs. 3(a)–3(b) refer to the summer and winter scenarios respectively, assuming that (i) no PV systems are installed (plots on the left) and (ii) about 30% of users are equipped with PV generators (plots on the right).

In all cases, the effect of smart EV charging is twofold, i.e., power consumption peak shaving and reverse power flow prevention. The latter effect is especially visible when the effect of PV penetration is stronger (i.e., in the summer season), and it confirms the correct operation of the optimisation algorithm, since it still handles the reverse power flows quite well.

The efficiency of the proposed V2G-based smart EV charging policy is assessed in terms of relative NLV reduction (NLVR) with respect to the scenario in which no smart EV charging is used.

Figs. 4(a) and 4(b) show the contour lines of the NLVR surfaces as a function of both PV_{share} and EV_{share} in the summer and winter scenarios, respectively. These diagrams quantify the joint effect of EV and PV penetration in ideal conditions (i.e., when a perfect schedule is possible), thus highlighting the operating conditions that maximise the NLVR. Indeed, up to about 60% NLVR could potentially be reached in both the summer and winter scenarios, although the pair of PV_{share} and EV_{share} values that best minimises the NLVR strongly depends on the season. The contour lines in the winter scenario indeed just look like a zoomed view of those on the left side of the plot in the summer case. This is simply due to the fact that in winter, a much larger PV penetration would be needed to reach the same NLVR values seen in summer. Quite interestingly, if no PV generators at all are deployed, the maximum NLVR (between 50% and 55% in both seasons) in the case at hand is reached if EV_{share} is about 30%. While these

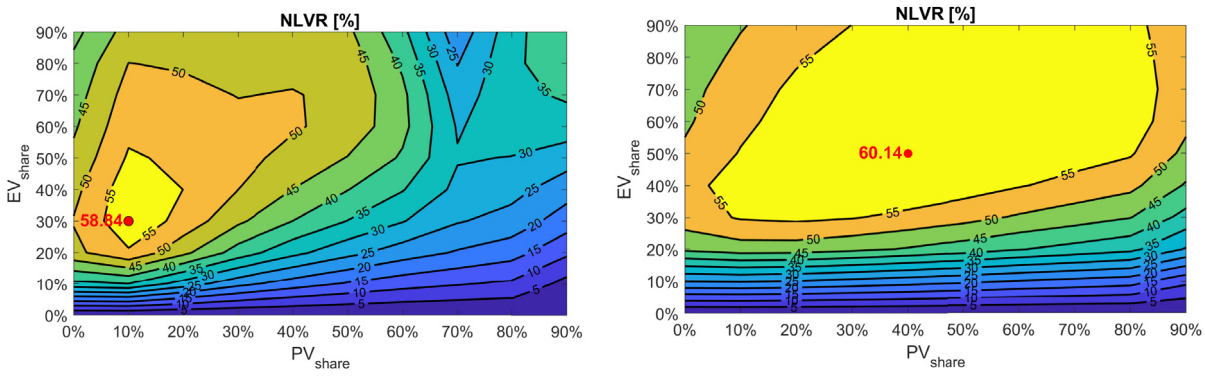

(a) Summer (b) Winter

Fig. 4. Ideal contour curves of the NLVR surfaces as a function of increasing shares of users equipped with PV systems and/or EVs in summer (a) and winter (b), respectively. Results are computed in ideal conditions, i.e. assuming that the user behaviour's and profile is exactly the same as expected.

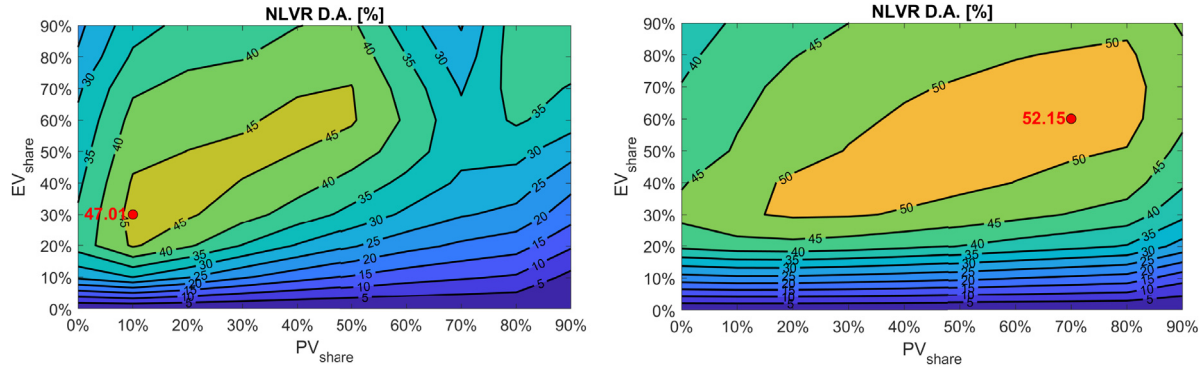

(a) Summer (b) Winter

Fig. 5. Contour curves of the NLVR surfaces obtained assuming a basic day-ahead persistence model of PV generation and load profiles as a function of increasing shares of users equipped with PV systems and/or EVs in summer (a) and winter (b), respectively. In this case, the EVs charging profiles computed over a given day are applied to the following day. However, the constraints due to the unavailability of different EVs at different times of the day override the V charging schedule.

numbers depend on the specific case study considered, this result is very important because it confirms that the optimal V2G-based EV charging scheme is potentially very effective, regardless of whether the distributed generators are installed or not. The effect of PV generators is twofold. To a certain extent (e.g., when PV_{share} does not exceed 40%) the PV generators support the increasing electricity demand due to EVs if EV_{share} grows, thus contributing to the net-load variance reduction provided by the V2G-based EV charging policy. However, if PV_{share} increases excessively and is not supported by an increase in EV_{share}, the NLVR sharply decreases in summer, because the overall net-load is so heavily affected by the reverse power flows, that the EVs are no longer able to handle the PV overproduction.

Figs. 5(a) and 5(b) show the NLVR contour lines computed when the optimal V2G-based EV charging schedule is based on the load and PV generation profiles of the previous day (persistence model). This model is straightforward to apply and suitable to test the impact of the smart EV charging algorithm on NLVR in more realistic conditions, namely when the load, the PV generation, and the EV usage conditions significantly differ from the expected ones. The persistence model provides a reasonable lower bound for the algorithm performance evaluation. Indeed, the contour curves in Figs. 5(a) and 5(b) are qualitatively similar to those in Figs. 4(a) and 4(b), but the NLVR surfaces when the persistence model is used decrease by about 10% compared to the ideal case in both summer and winter (the NLVR peaks are around 50%). This is nonetheless a remarkable result, especially given the broad range of PV_{share} and EV_{share} values. In conclusion, the presented analysis clearly shows that, in all cases, a good mitigation of the net-load variance can be obtained if at least 20% of users own an EV. Moreover, the net-load variance is dominated by the PV reverse power flows and it can be hardly reduced by the proposed V2G EV smart charging policy (especially in summer) when PV_{share} exceeds 50% and EV_{share} is lower than about 30%.

6. Impact analysis

Since the implications of smart EV battery charging are wider than just active power support, the results of additional simulations are presented in this Section. Such simulations provide an overview of the impact of the proposed smart EV charging policy on district-level energy independence, grid voltage stability and lines congestion, and EVs' battery wear. All results are obtained in realistic conditions, i.e., when the day-ahead persistence forecasting model is applied.

6.1. Energy independence analysis

Several Authors found that smart EV charging is useful to increase district self-consumption (SC) and self-production (SP) [66,67]. SC expresses how efficient a system is in consuming or storing the generated PV energy, whereas SP represents the fraction of the total appliances and EV consumption that is covered by proprietary PV production. In principle, both indexes should be maximised, in accordance with the concept of net-zero energy districts [83], but it is realistically not always possible because, for

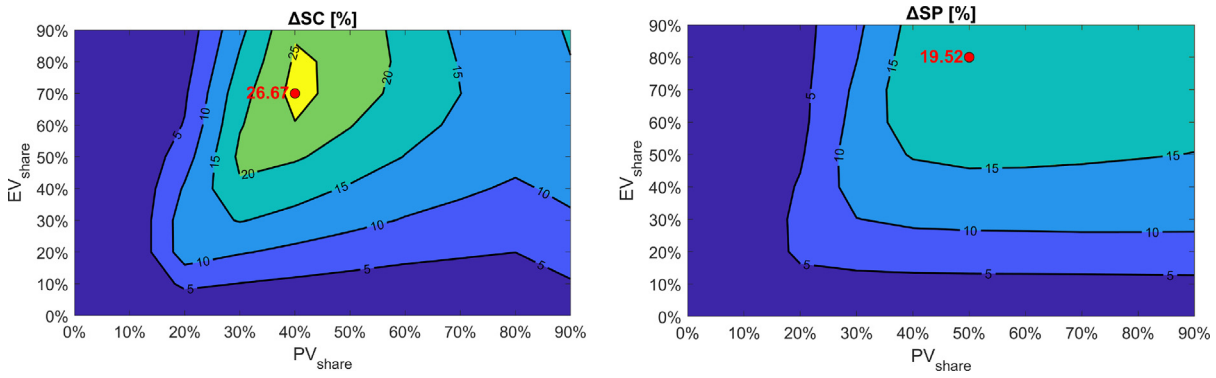

Fig. 6. Increments of the district-level self-consumption (*SC*) (a) and self-production (*SP*) values (b) due to the proposed EV smart charging policy in the summer scenario.

instance, an increase in PV_{share} with a constant EV_{share} decreases *SC* and increases *SP* at the same time. The total relative *SC* and *SP* increments at the district level obtained by adopting the proposed smart EV charging policy are shown in Fig. 6(a)–(b) in the summer scenario. The results in winter are qualitatively similar, but milder. Therefore, they are omitted for the sake of brevity.

Not surprisingly, the highest *SC* and *SP* increments are obtained for a pair of (PV_{share}, EV_{share}) values quite different from those corresponding to the NLVR maxima in Figs. 5(a) and 5(b), i.e. (40%, 70%) in Fig. 6(a) and (50%, 80%) in Fig. 6(b). This is due to the fact that an algorithm aimed at smoothing the NLV can help but is not conceived to maximise the exploitation of the available solar energy. Even if it is not shown in the paper, the baseline maximum SC and SP values are around 50%. Hence, half of the PV generated energy is either consumed or stored in the EVs and half of the total load demand is covered by PV. Based on that, the shown increases in *SC* and *SP* just by smart charging the EVs (no stationary storage required) are quite remarkable. Once again, we can conclude that the benefits of jointly increasing PV and EV penetration are generally well visible. Interestingly enough, the increment in *SC* can be up to a few percent points higher than the *SP* one, meaning that the smart EV charging is slightly more effective in smoothing the reverse power flows, rather than handling excessive load peaks.

6.2. Bus voltage stability and lines congestion

The correct and stable operation of the IEEE 906-bus LV distribution system used as a case study was checked through repeated three-phase power flow analyses based on the classic Newton-Raphson method implemented in OpenDSS[7] for increasing values of PV_{share} and EV_{share} with and without using the V2G-based smart EV charging policy. Given that the distribution system under test is supposed to operate in almost balanced conditions, due to the reasons explained in Sections 4.2–4.4, the bars representing the range (with 99% probability) of bus voltage amplitude variations shown in Fig. 7 refer to the positive sequence bus voltages only, over the whole grid in a typical summer week (i.e., in the worst case due to the large amount of generated PV power) for different levels of PV_{share} and EV_{share}. In particular, each triplet of bars in Fig. 7 represents the range of bus voltages obtained respectively (from left to right) in the baseline case (i.e., without considering the EVs), including the additional load due to standard EVs charging (i.e., at the maximum possible rate), and by using the proposed V2G-based smart EV charging algorithm.

As it can be easily seen, if $PV_{share} = 90\%$ the $\pm 10\%$ upper and lower voltage limits recommended in [18] are exceeded both without EVs and when the EVs are charged with the standard approach. This is due mainly to the reverse power flows caused by the surplus of generated PV power. On the contrary, the V2G-based smart EV charging policy tends to better exploit the available PV power, with an evident reduction of the range of bus voltage fluctuations. In particular, in this case the voltage amplitude values are generally confined within the $\pm 10\%$ limits (with a few exceptions), since it is not possible to fully control the voltage values at all buses (as explained in Section 3) when the number of (controllable) EV charging stations is small compared to the share of users equipped with PV generators. The stabilising action of the V2G-based approach becomes more and more evident as the values of EV_{share} and PV_{share} grow. The additional load due to standard EV charging may cause a much higher risk of under-voltages (i.e., below the 0.9 p.u. limit specified in [18]) especially if such additional load is not at least partially supplied by PV generators. In this case, the lower voltage limit is clearly exceeded even when $EV_{share} = 30\%$. The V2G-based smart EV charging policy strongly reduces the risk of such events, which become negligible when at least 60% of users own an EV.

In order to analyse the impact of the proposed solution on grid congestion issues, Fig. 8 shows the range (with 99% probability) of the line current values normalised by the respective ampacities in a typical summer week. Again, the bar diagrams are plotted for different levels of PV penetration and for increasing values of EV_{share}. The meaning of the triplets of bars in each plot is the same as in Fig. 7.

Quite interestingly, when $PV_{share} \geq 60\%$, a high production–consumption simultaneity is noted, so the EVs are naturally recharged by the PV generators, and the smart EV charging is less effective in reducing the grid congestion levels. In any case, the benefit of the proposed policy is quite evident, and it becomes more effective when the values of EV_{share} and PV_{share} grow. In this case, the peak line currents may be reduced by more than 50%.

6.3. Battery wear analysis

One of the strongest criticisms to V2G-based EV charging policies is the actual stress on EVs' batteries, whose lifetime might be significantly reduced by the larger number of charging and discharging cycles. The relative reduction of the battery capacity of the $j-$th EV consists of two contributions [84,85], i.e., $\frac{\Delta C_j}{C_j}(y, T_K) = \frac{\Delta C_j^{CAL}}{C_j}(y, T_K) + \frac{\Delta C_j^{CYC}}{C_j}(y, T_K)$, where y represents the years of battery use, T_K is the average battery pack temperature

$$\frac{\Delta C_j^{CAL}}{C_j}(y, T_K) = \alpha_{CAL} \cdot e^{\beta_{CAL} \cdot T_K} \cdot (y \cdot 12)^{0.5} \tag{13}$$

[7] OpenDSS: Open Distribution System Simulator v9.0.0, R. Dugan, D. Montenegro, A. Ballanti, https://www.epri.com/pages/sa/opendss

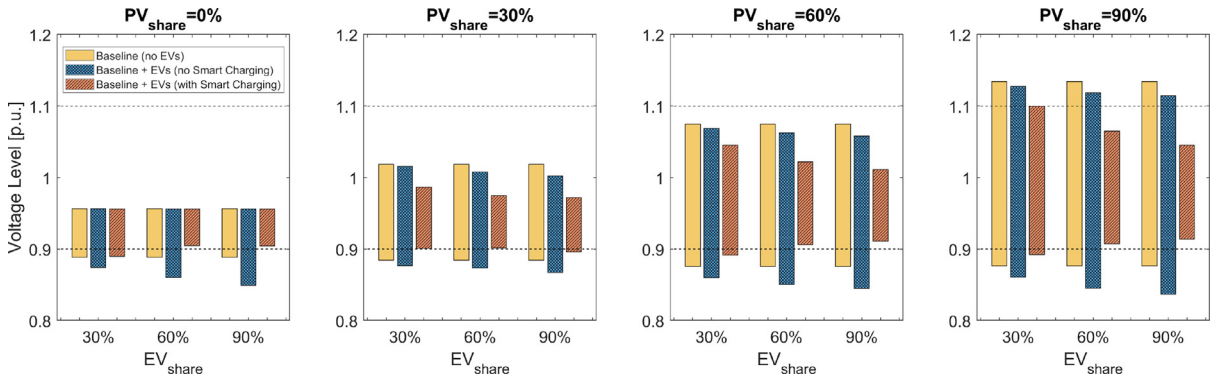

Fig. 7. Range (with 99% probability) of the bus voltage amplitude values in a typical summer week for increasing levels of PV and EV penetration. Each triple of bars includes: the baseline case (i.e., without considering the EVs), the case when the additional load due to standard EVs charging is considered, and the dual results obtained by using the V2G-based smart EV charging algorithm.

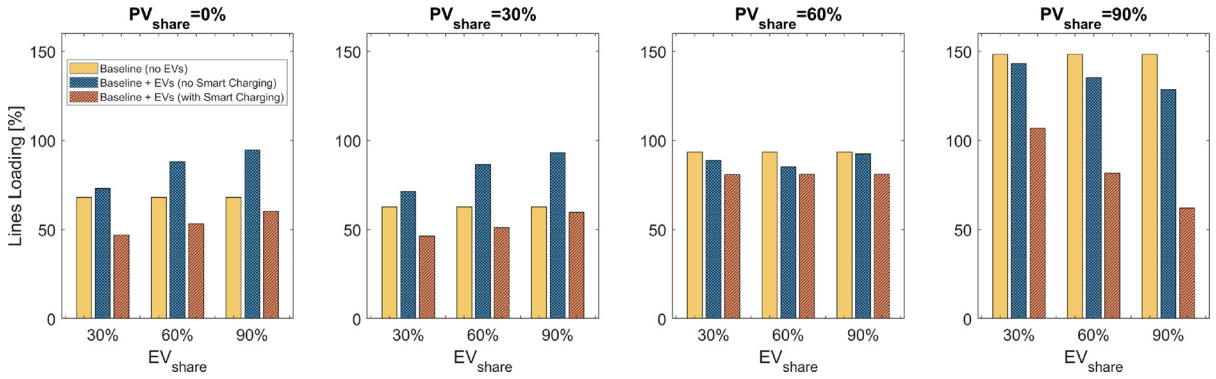

Fig. 8. Range (with 99% probability) of the lines current loading values normalised by their respective ampacity in a typical summer week for increasing levels of PV and EV penetration. Each triplet of bars includes: the baseline case (i.e., without considering the EVs), the case when the additional load due to standard EVs charging is considered, and the dual results obtained by using the V2G-based smart EV charging algorithm.

is the capacity reduction due to the pure calendar-time ageing and

$$\frac{\Delta C_j^{CYC}}{C_j}(y, T_K) = \alpha_{CYC} \cdot e^{\beta_{CYC} \cdot T_K} \cdot (NC_j^{EQ})^{0.5} \cdot y \tag{14}$$

is the contribution due to the charging–discharging cycling effect, with NC_j^{EQ} being indeed is the number of equivalent full charging and discharging cycles.

Both expressions (13) and (14) are empirical and rely on coefficients that are estimated experimentally [85]. In particular, in the case at hand

- the coefficients $\alpha_{CAL} = 1.985 \cdot 10^{-7}$, $\beta_{CAL} = 0.0510\ \mathrm{K}^{-1}$, $\alpha_{CYC} = 4.42 \cdot 10^{-5}$, and $\beta_{CYC} = 0.02676\ \mathrm{K}^{-1}$ are based on some tests on Li-ion batteries for EVs [84].
- $T_K = 304$ K (i.e., 31 °C). Even if EVs cannot not be charged always at the same temperature, this is a conservative value which includes also the raise over the environmental temperature just due to charging (e.g., about 10 °C for the full recharge of a 60 kW h battery when a 3.7 kW station is used [86]).
- The NC_j^{EQ} values were estimated with the Palmgren-Miner rule [84].

The total battery lifetime is estimated by computing the value of y for which $\frac{\Delta C_j}{C_j} = 20\%$ given by the sum of (13) and (14), which is a conservative, but realistic assumption [84]. This assumption is equal to setting SOH = 80% as the minimum allowable state-of-health of the battery, i.e., the capacity left after y years compared to the original capacity C. Fig. 9 shows the box-and-whiskers plots of the total relative EV battery lifetime reduction caused by the proposed V2G-based smart charging policy. Since the number of full charging and discharging cycles NC_j^{EQ} highly depends on battery capacity, the results of PHEVs only (8–10 kW h) are presented, because the BEVs never reach the end-of-life in the simulated 10 years of EV time span. Both box-and-whiskers plots are reported for increasing values of EV_{share} and PV_{share}.

A first noticeable difference between PHEVs and BEVs is that, for the same values of EV_{share} and PV_{share}, the median value of the battery lifetime reduction of the majority of PHEVs is much higher than in the BEVs case (10%–20% instead of 0%–5%). This is due to the much smaller size of PHEVs' batteries, which causes a larger number of full charging–discharging cycles NC_j^{EQ} when the V2G-based EV charging policy is applied. Noticeable max reductions of 35% are shown for PHEVs, whereas for BEVs this value is around 30%. Interestingly enough, the interquartile range of BEVs' battery lifetime reduction is instead quite larger than in the PHEV case, because of the broader range of possible C_j values, which affects the variability of NC_j^{EQ} as well.

7. Conclusions and future work

In this work, a centralised V2G-based smart EV charging algorithm aimed at reducing the net-load variance by leveraging the EV charging stations is proposed. The algorithm performance was analysed by increasing both the number of users equipped with an EV charging station and the PV penetration level. The optimal scheduling problem was solved through quadratic programming, while keeping into consideration a variety of user-driven and grid-related constraints, such as the bus voltage limitations.

The optimisation results show sizeable benefits if the PV and EV penetration levels are simultaneously increased, so the local

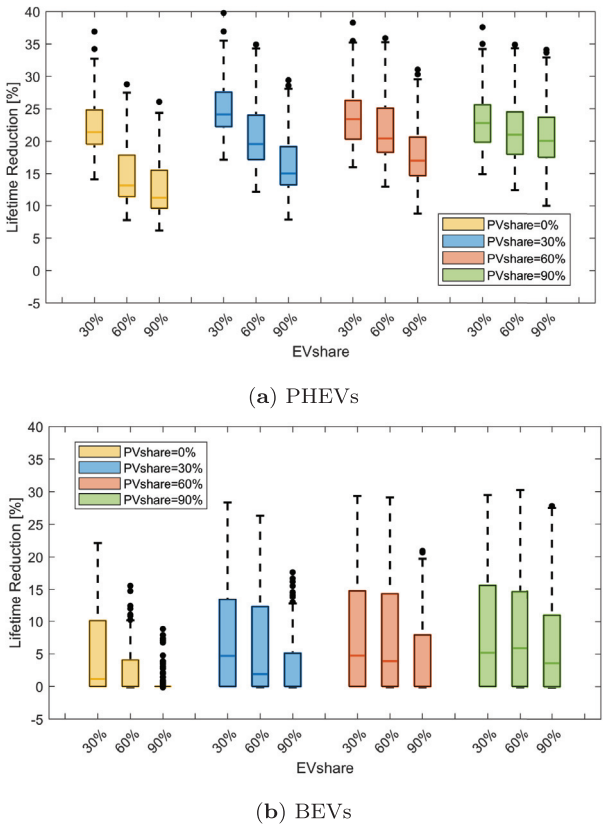

(a) PHEVs

(b) BEVs

Fig. 9. Distribution of the relative lifetime reduction of PHEVs and BEVs due to the application of the proposed V2G-based smart EV charging algorithm.

generation supports the additional EV demand. In such conditions, the overall net-load variance over the considered distribution grid can be reduced up to about 60% in ideal conditions, or about 50% when a basic persistence forecasting model of loads and PV generation profiles is used. Thanks to V2G-based smart EV charging, self-consumption and self-production increments by up to 27% and 20% respectively, are attainable at the district level. However, such benefits decrease if the distributed PV generation is excessive, since the EV smart scheduling cannot efficiently manage a large PV overproduction. This does not depend on the scheduling algorithm per se, but on the baseline operating conditions of the grid. In general, the V2G-based smart EV charging scheme has also a positive impact on grid voltage stability and lines congestion, as confirmed by the negligible amount of over-voltage, under-voltage and over-current events. Finally, a preliminary battery wear analysis shows that, in this specific case study, V2G-based smart EV charging may significantly reduce the battery lifetime, with the BEVs suffering much less than PHEVs due to their larger battery capacity and lower cycling ageing.

This paper analyses the potential for active power support with centralised smart EV charging when the coordinator has full access to the information regarding the EVs connecting to the system. Hence, future work may try to address this limitation. Firstly, the optimisation could be done by including more effective forecasting techniques in the case of missing information on loads and generators. Secondly, a solution to address the EV smart charging problem in real-time could be devised. Finally, a future work should try to analyse the economic benefits for the EV owners and DSOs that participate in a smart EV charging program, considering different compensation schemes.

CRediT authorship contribution statement

M. Secchi: Conceptualization, Methodology, Formal analysis, Validation, Software, Writing – original draft. **G. Barchi:** Conceptualization, Methodology, Validation, Writing – review & editing, Supervision. **D. Macii:** Conceptualization, Methodology, Formal analysis, Validation, Writing – original draft. **D. Petri:** Writing – review & editing, Supervision.

Declaration of competing interest

The authors declare that they have no known competing financial interests or personal relationships that could have appeared to influence the work reported in this paper.

Data availability

Data will be made available on request.

Acknowledgements

The Authors would like to thank the Department of Innovation, Research and University of the Autonomous Province of Bozen/Bolzano for covering the Open Access publication costs.

References

[1] European Commission, E. Commission, Fit for 55 - EU commission legislative train schedule, 2021, URL https://www.europarl.europa.eu/legislative-train/theme-a-european-green-deal/package-fit-for-55.

[2] IRENA, World Energy Transitions Outlook: 1.5° C Pathway, Tech. Rep., IRENA, 2021, p. 58, URL https://www.irena.org/publications/2021/Jun/World-Energy-Transitions-Outlook.

[3] B. Xu, A. Sharif, M. Shahbaz, K. Dong, Have electric vehicles effectively addressed CO2 emissions? Analysis of eight leading countries using quantile-on-quantile regression approach, Sustain. Prod. Consumpt. 27 (2021) 1205–1214, http://dx.doi.org/10.1016/j.spc.2021.03.002.

[4] M.M. Rahman, Y. Zhou, J. Rogers, V. Chen, M. Sattler, K. Hyun, A comparative assessment of CO2 emission between gasoline, electric, and hybrid vehicles: A Well-To-Wheel perspective using agent-based modeling, J. Clean. Prod. 321 (October 2020) (2021) 128931, http://dx.doi.org/10.1016/j.jclepro.2021.128931.

[5] M.E. Biresselioglu, M. Demirbag Kaplan, B.K. Yilmaz, Electric mobility in Europe: A comprehensive review of motivators and barriers in decision making processes, Transp. Res. A 109 (2018) 1–13, http://dx.doi.org/10.1016/J.TRA.2018.01.017.

[6] M. Secchi, G. Barchi, D. Macii, D. Moser, D. Petri, Multi-objective battery sizing optimisation for renewable energy communities with distribution-level constraints: A prosumer-driven perspective, Appl. Energy 297 (2021) 117171, http://dx.doi.org/10.1016/J.APENERGY.2021.117171.

[7] G. Barchi, D. Macii, A photovoltaics-aided interlaced extended Kalman filter for distribution systems state estimation, Sustain. Energy Grids Netw. 26 (2021) 100438, http://dx.doi.org/10.1016/j.segan.2021.100438.

[8] S. Johansson, J. Persson, S. Lazarou, A. Theocharis, Investigation of the impact of large-scale integration of electric vehicles for a Swedish distribution network, Energies 2019, Vol. 12, Page 4717 12 (24) (2019) 4717, http://dx.doi.org/10.3390/EN12244717.

[9] A.A.R. Mohamed, R.J. Best, D.J. Morrow, A. Cupples, I. Bailie, Impact of the deployment of solar photovoltaic and electrical vehicle on the low voltage unbalanced networks and the role of battery energy storage systems, J. Energy Storage 42 (2021) 102975, http://dx.doi.org/10.1016/J.EST.2021.102975.

[10] R. Fachrizal, U.H. Ramadhani, J. Munkhammar, J. Widén, Combined PV–EV hosting capacity assessment for a residential LV distribution grid with smart EV charging and PV curtailment, Sustain. Energy Grids Netw. 26 (2021) 100445, http://dx.doi.org/10.1016/J.SEGAN.2021.100445.

[11] L.I. Dulau, D. Bica, Effects of electric vehicles on power networks, Procedia Manuf. 46 (2020) 370–377, http://dx.doi.org/10.1016/J.PROMFG.2020.03.054.

[12] R. Saravanan, S. Kaliappan, V. Jayaprakasan, P. Maniraj, A hybrid strategy for mitigating unbalance and improving voltage considering higher penetration of electric vehicles and distributed generation, Sustainable Cities Soc. 76 (2022) 103489, http://dx.doi.org/10.1016/J.SCS.2021.103489.

[13] M.R. Islam, H. Lu, M.J. Hossain, L. Li, Optimal coordination of electric vehicles and distributed generators for voltage unbalance and neutral current compensation, IEEE Trans. Ind. Appl. 57 (1) (2021) 1069–1080, http://dx.doi.org/10.1109/TIA.2020.3037275.

[14] J. Guo, H. Zhao, Z. Shen, A. Wang, L. Cao, E. Hu, Z. Wang, X. Song, Research on harmonic characteristics and harmonic counteraction problem of EV charging station, in: 2nd IEEE Conference on Energy Internet and Energy System Integration, EI2 2018 - Proceedings, Institute of Electrical and Electronics Engineers Inc., 2018, http://dx.doi.org/10.1109/EI2.2018.8582095.

[15] C. Biedermann, G.-L. Di Modica, B. Engel, Measurement of the voltage quality and load profiles of electric vehicles, in: CIRED 2021 - the 26th International Conference and Exhibition on Electricity Distribution, Institution of Engineering and Technology (IET), 2022, pp. 891–895, http://dx.doi.org/10.1049/ICP.2021.2162.

[16] B. Basta, W.G. Morsi, Probabilistic assessment of the impact of integrating large-scale high-power fast charging stations on the power quality in the distribution systems, in: 2020 IEEE Electric Power and Energy Conference, EPEC 2020, Institute of Electrical and Electronics Engineers Inc., 2020, http://dx.doi.org/10.1109/EPEC48502.2020.9320013.

[17] S.M. Alshareef, W.G. Morsi, Impact of fast charging stations on the voltage flicker in the electric power distribution systems, in: 2017 IEEE Electrical Power and Energy Conference, Vol. 2017-October, EPEC 2017, Institute of Electrical and Electronics Engineers Inc., 2018, pp. 1–6, http://dx.doi.org/10.1109/EPEC.2017.8286226.

[18] Voltage characteristics of electricity supplied by public distribution networks, 2010, EN 50160:2010.

[19] A.F. Cortés Borray, J. Merino, E. Torres, A. Garcés, J. Mazón, A.F.C. Borray, J. Merino, E. Torres, A. Garcés, J. Mazón, A.F. Cortés Borray, J. Merino, E. Torres, A. Garcés, J. Mazón, Centralised coordination of EVs charging and PV active power curtailment over multiple aggregators in low voltage networks, Sustain. Energy Grids Netw. 27 (2021) 100470, http://dx.doi.org/10.1016/j.segan.2021.100470.

[20] F. Palmiotto, Y. Zhou, G. Forte, M. Dicorato, M. Trovato, L.M. Cipcigan, A coordinated optimal programming scheme for an electric vehicle fleet in the residential sector, Sustain. Energy Grids Netw. 28 (2021) 100550, http://dx.doi.org/10.1016/j.segan.2021.100550.

[21] B. Bibak, H. Tekiner-Mogulkoc, Influences of vehicle to grid (V2G) on power grid: An analysis by considering associated stochastic parameters explicitly, Sustain. Energy Grids Netw. 26 (2021) 100429, http://dx.doi.org/10.1016/j.segan.2020.100429.

[22] R.N.E. Idrissi, M. Ouassaid, M. Maaroufi, A constrained programming-based algorithm for optimal scheduling of aggregated EVs power demand in smart buildings, IEEE Access 10 (2022) 28434–28444, http://dx.doi.org/10.1109/ACCESS.2022.3154781.

[23] C.S. Ioakimidis, D. Thomas, P. Rycerski, K.N. Genikomsakis, Peak shaving and valley filling of power consumption profile in non-residential buildings using an electric vehicle parking lot, Energy 148 (2018) 148–158, http://dx.doi.org/10.1016/j.energy.2018.01.128.

[24] P. Huang, R. Tu, X. Zhang, M. Han, Y. Sun, S.A. Hussain, L. Zhang, Investigation of electric vehicle smart charging characteristics on the power regulation performance in solar powered building communities and battery degradation in Sweden, J. Energy Storage 56 (2022) 105907, http://dx.doi.org/10.1016/J.EST.2022.105907.

[25] E. Hadian, H. Akbari, M. Farzinfar, S. Saeed, Optimal allocation of electric vehicle charging stations with adopted smart charging/discharging schedule, IEEE Access 8 (2020) 196908–196919, http://dx.doi.org/10.1109/ACCESS.2020.3033662.

[26] S. Abdullah-Al-Nahid, T.A. Khan, M.A. Taseen, T. Jamal, T. Aziz, A novel consumer-friendly electric vehicle charging scheme with vehicle to grid provision supported by genetic algorithm based optimization, J. Energy Storage 50 (2022) 104655, http://dx.doi.org/10.1016/J.EST.2022.104655.

[27] M. Alonso, H. Amaris, J.G. Germain, J.M. Galan, Optimal charging scheduling of electric vehicles in smart grids by heuristic algorithms, Energies 7 (2014) 2449–2475, http://dx.doi.org/10.3390/en7042449.

[28] S. Li, C. Gu, X. Zeng, P. Zhao, X. Pei, S. Cheng, Vehicle-to-grid management for multi-time scale grid power balancing, Energy 234 (2021) 121201, http://dx.doi.org/10.1016/j.energy.2021.121201.

[29] M.E. Gerards, J.L. Hurink, Robust peak-shaving for a neighborhood with electric vehicles, Energies 9 (2016) 594, http://dx.doi.org/10.3390/EN9080594.

[30] S.U. Khan, K.K. Mehmood, Z.M. Haider, M.K. Rafique, M.O. Khan, C.H. Kim, Coordination of multiple electric vehicle aggregators for peak shaving and valley filling in distribution feeders, Energies 14 (2021) 352, http://dx.doi.org/10.3390/EN14020352.

[31] R. Garruto, M. Longo, W. Yaïci, F. Foiadelli, Connecting parking facilities to the electric grid: A vehicle-to-grid feasibility study in a railway station's car park, Energies 13 (2020) 3083, http://dx.doi.org/10.3390/EN13123083.

[32] M.J. Alam, K.M. Muttaqi, D. Sutanto, A Controllable local peak-shaving strategy for effective utilization of PEV battery capacity for distribution network support, IEEE Trans. Ind. Appl. 51 (3) (2015) 2030–2037, http://dx.doi.org/10.1109/TIA.2014.2369823.

[33] M. Arnaudo, M. Topel, B. Laumert, Vehicle-to-grid for peak shaving to unlock the integration of distributed heat pumps in a Swedish neighborhood, Energies 13 (2020) 1705, http://dx.doi.org/10.3390/EN13071705.

[34] M.C. Kisacikoglu, F. Erden, N. Erdogan, Distributed control of PEV charging based on energy demand forecast, IEEE Trans. Ind. Inform. 14 (2018) 332–341, http://dx.doi.org/10.1109/TII.2017.2705075.

[35] K. Mahmud, M.J. Hossain, G.E. Town, Peak-load reduction by coordinated response of photovoltaics, battery storage, and electric vehicles, IEEE Access 6 (2018) 29353–29365, http://dx.doi.org/10.1109/ACCESS.2018.2837144.

[36] M. Dorokhova, Y. Martinson, C. Ballif, N. Wyrsch, Deep reinforcement learning control of electric vehicle charging in the presence of photovoltaic generation, Appl. Energy 301 (2021) 117504, http://dx.doi.org/10.1016/J.APENERGY.2021.117504.

[37] X. Yang, Y. Zhang, F. Zhang, C. Xu, B. Yi, Enhancing utilization of PV energy in building microgrids via autonomous demand response, IEEE Access 9 (2021) 23554–23564, http://dx.doi.org/10.1109/ACCESS.2021.3052521.

[38] N. Liu, Q. Chen, J. Liu, X. Lu, P. Li, J. Lei, J. Zhang, A heuristic operation strategy for commercial building microgrids containing EVs and PV system, IEEE Trans. Ind. Electron. 62 (4) (2015) 2560–2570, http://dx.doi.org/10.1109/TIE.2014.2364553.

[39] Y. Hu, M. Zhang, K. Wang, D.Y. Wang, Optimization of orderly charging strategy of electric vehicle based on improved alternating direction method of multipliers, J. Energy Storage 55 (2022) 105483, http://dx.doi.org/10.1016/J.EST.2022.105483.

[40] J. Rivera, C. Goebel, H.A. Jacobsen, Distributed convex optimization for electric vehicle aggregators, IEEE Trans. Smart Grid 8 (2017) 1852–1863, http://dx.doi.org/10.1109/TSG.2015.2509030.

[41] D. Liu, T. Zhang, W. Wang, X. Peng, M. Liu, H. Jia, S. Su, Two-stage physical economic adjustable capacity evaluation model of electric vehicles for peak shaving and valley filling auxiliary services, Sustainability 2021, Vol. 13, Page 8153 13 (2021) 8153, http://dx.doi.org/10.3390/SU13158153.

[42] M. Shibl, L. Ismail, A. Massoud, Electric vehicles charging management using machine learning considering fast charging and vehicle-to-grid operation, Energies 14 (2021) 6199, http://dx.doi.org/10.3390/EN14196199.

[43] Y. Shang, M. Liu, Z. Shao, L. Jian, Internet of smart charging points with photovoltaic integration: A high-efficiency scheme enabling optimal dispatching between electric vehicles and power grids, Appl. Energy 278 (2020) 115640, http://dx.doi.org/10.1016/J.APENERGY.2020.115640.

[44] M.F. El-Naggar, A.A.A. Elgammal, Multi-objective optimal predictive energy management control of grid-connected residential wind-PV-FC-battery powered charging station for plug-in electric vehicle, J. Electr. Eng. Technol. 13 (2) (2018) 742–751, http://dx.doi.org/10.5370/JEET.2018.13.2.742.

[45] W. Jiang, Y. Zhen, A real-time EV charging scheduling for parking lots with PV system and energy store system, IEEE Access 7 (2019) 86184–86193, http://dx.doi.org/10.1109/ACCESS.2019.2925559.

[46] V.K. Jadoun, N. Sharma, P. Jha, N.S. Jayalakshmi, H. Malik, F.P.G. Márquez, Optimal scheduling of dynamic pricing based V2G and G2V operation in microgrid using improved elephant herding optimization, Sustainability 13 (2021) 7551, http://dx.doi.org/10.3390/SU13147551.

[47] J. Yang, L. He, S. Fu, An improved PSO-based charging strategy of electric vehicles in electrical distribution grid, Appl. Energy 128 (2014) 82–92, http://dx.doi.org/10.1016/j.apenergy.2014.04.047.

[48] J. Yang, W. Wang, K. Ma, B. Yang, Optimal dispatching strategy for shared battery station of electric vehicle by divisional battery control, IEEE Access 7 (2019) 38224–38235, http://dx.doi.org/10.1109/ACCESS.2019.2906488.

[49] S. Englberger, K.A. Gamra, B. Tepe, M. Schreiber, A. Jossen, H. Hesse, Electric vehicle multi-use: Optimizing multiple value streams using mobile storage systems in a vehicle-to-grid context, Appl. Energy 304 (2021) 117862, http://dx.doi.org/10.1016/J.APENERGY.2021.117862.

[50] A. Ouammi, Peak loads shaving in a team of cooperating smart buildings powered solar PV-based microgrids, IEEE Access 9 (2021) 24629–24636, http://dx.doi.org/10.1109/ACCESS.2021.3057458.

[51] A. Tchagang, Y. Yoo, V2B/V2G on energy cost and battery degradation under different driving scenarios, peak shaving, and frequency regulations, World Electr. Veh. J. 2020, Vol. 11, Page 14 11 (2020) 14, http://dx.doi.org/10.3390/WEVJ11010014.

[52] B. Sun, Z. Huang, X. Tan, D.H. Tsang, Optimal scheduling for electric vehicle charging with discrete charging levels in distribution grid, IEEE Trans. Smart Grid 9 (2018) 624–634, http://dx.doi.org/10.1109/TSG.2016.2558585.

[53] S. Shi, C. Fang, H. Wang, J. Li, Y. Li, D. Peng, H. Zhao, Two-step intelligent control for a green flexible EV energy supply station oriented to dual carbon targets, Processes 9 (2021) 1918, http://dx.doi.org/10.3390/PR9111918.

[54] F. Hafiz, A.R.D. Queiroz, I. Husain, Coordinated control of PEV and PV-based storages in residential systems under generation and load uncertainties, IEEE Trans. Ind. Appl. 55 (2019) 5524–5532, http://dx.doi.org/10.1109/TIA.2019.2929711.
[55] J. García-Villalobos, I. Zamora, K. Knezović, M. Marinelli, Multi-objective optimization control of plug-in electric vehicles in low voltage distribution networks, Appl. Energy 180 (2016) 155–168, http://dx.doi.org/10.1016/j.apenergy.2016.07.110.
[56] M. van der Kam, W. van Sark, M.V.D. Kam, W.V. Sark, Smart charging of electric vehicles with photovoltaic power and vehicle-to-grid technology in a microgrid; a case study, Appl. Energy 152 (2015) 20–30, http://dx.doi.org/10.1016/j.apenergy.2015.04.092.
[57] D.V.D. Meer, G.R.C. Mouli, G. Morales-España, L.R. Elizondo, P. Bauer, Energy management system with PV power forecast to optimally charge EVs at the workplace, IEEE Trans. Ind. Inform. 14 (1) (2018) 311–320, http://dx.doi.org/10.1109/TII.2016.2634624.
[58] Y. Achour, A. Ouammi, D. Zejli, Model predictive control based demand response scheme for peak demand reduction in a smart campus integrated microgrid, IEEE Access 9 (2021) 162765–162778, http://dx.doi.org/10.1109/ACCESS.2021.3132895.
[59] Y.L. Lou, C.X. Wu, Z.Z. Shi, R. Yang, Evaluation of EV penetration level limit in distribution system applying charging and scheduling strategies, Sustain. Energy Grids Netw. 32 (2022) 100922, http://dx.doi.org/10.1016/J.SEGAN.2022.100922.
[60] M.S. Hashim, J.Y. Yong, V.K. Ramachandaramurthy, K.M. Tan, M. Mansor, M. Tariq, Priority-based vehicle-to-grid scheduling for minimization of power grid load variance, J. Energy Storage 39 (2021) 102607, http://dx.doi.org/10.1016/j.est.2021.102607.
[61] Z. Yu, P. Gong, Z. Wang, Y. Zhu, R. Xia, Y. Tian, Real-time control strategy for aggregated electric vehicles to smooth the fluctuation of wind-power output, Energies 13 (2020) 757, http://dx.doi.org/10.3390/EN13030757.
[62] S.U. Khan, K.K. Mehmood, Z.M. Haider, M.K. Rafique, C.H. Kim, A bi-level EV aggregator coordination scheme for load variance minimization with renewable energy penetration adaptability, Energies 11 (2018) 2809, http://dx.doi.org/10.3390/EN11102809.
[63] R. Ghotge, Y. Snow, S. Farahani, Z. Lukszo, A. van Wijk, Optimized scheduling of EV charging in solar parking lots for local peak reduction under EV demand uncertainty, Energies 13 (5) (2020) 1275, http://dx.doi.org/10.3390/en13051275.
[64] B. Hu, S. Wang, X. Zhang, T. Wang, F. Qu, W. Zheng, B. Zhou, Power grid peak shaving strategies based on electric vehicles and thermal storage electric boilers, in: IOP Conference Series: Earth and Environmental Science, Vol. 227, Institute of Physics Publishing, 2019, 032026, http://dx.doi.org/10.1088/1755-1315/227/3/032026.
[65] S. Ahmadi, H.P. Arabani, D.A. Haghighi, J.M. Guerrero, Y. Ashgevari, A. Akbarimajd, Optimal use of vehicle-to-grid technology to modify the load profile of the distribution system, J. Energy Storage 31 (October 2019) (2020) 101627, http://dx.doi.org/10.1016/j.est.2020.101627.
[66] R. Fachrizal, J. Munkhammar, Improved photovoltaic self-consumption in residential buildings with distributed and centralized smart charging of electric vehicles, Energies 13 (5) (2020) 1153, http://dx.doi.org/10.3390/en13051153.
[67] R. Fachrizal, M. Shepero, M. Åberg, J. Munkhammar, Optimal PV-EV sizing at solar powered workplace charging stations with smart charging schemes considering self-consumption and self-sufficiency balance, Appl. Energy 307 (2022) 118139, http://dx.doi.org/10.1016/J.APENERGY.2021.118139.
[68] L. Jian, X. Zhu, Z. Shao, S. Niu, C.C. Chan, A scenario of vehicle-to-grid implementation and its double-layer optimal charging strategy for minimizing load variance within regional smart grids, Energy Convers. Manage. 78 (2014) 508–517, http://dx.doi.org/10.1016/j.enconman.2013.11.007.
[69] L. Jian, Y. Zheng, X. Xiao, C.C. Chan, Optimal scheduling for vehicle-to-grid operation with stochastic connection of plug-in electric vehicles to smart grid, Appl. Energy 146 (2015) 150–161, http://dx.doi.org/10.1016/j.apenergy.2015.02.030.
[70] G. Zhang, S.T. Tan, G.G. Wang, Real-time smart charging of electric vehicles for demand charge reduction at non-residential sites, IEEE Trans. Smart Grid 9 (2018) 4027–4037, http://dx.doi.org/10.1109/TSG.2016.2647620.
[71] A. Houbbadi, R. Trigui, S. Pelissier, E. Redondo-Iglesias, T. Bouton, Optimal scheduling to manage an electric bus fleet overnight charging, Energies 12 (14) (2019) 2727, http://dx.doi.org/10.3390/EN12142727.
[72] E.L. Karfopoulos, N.D. Hatziargyriou, Distributed coordination of electric vehicles providing V2G services, IEEE Trans. Power Syst. 31 (2016) 329–338, http://dx.doi.org/10.1109/TPWRS.2015.2395723.
[73] V. Marano, S. Onori, Y. Guezennec, G. Rizzoni, N. Madella, Lithium-ion batteries life estimation for plug-in hybrid electric vehicles, in: 5th IEEE Vehicle Power and Propulsion Conference, VPPC '09, 2009, pp. 536–543, http://dx.doi.org/10.1109/VPPC.2009.5289803.
[74] A. Hoke, A. Brissette, D. Maksimović, A. Pratt, K. Smith, Electric vehicle charge optimization including effects of lithium-ion battery degradation, in: 2011 IEEE Vehicle Power and Propulsion Conference, VPPC 2011, 2011, http://dx.doi.org/10.1109/VPPC.2011.6043046.
[75] V. Boglou, C.S. Karavas, K. Arvanitis, A. Karlis, A fuzzy energy management strategy for the coordination of electric vehicle charging in low voltage distribution grids, Energies 2020, Vol. 13, Page 3709 13 (14) (2020) 3709, http://dx.doi.org/10.3390/EN13143709.
[76] C. González-Morán, P. Arboleya, V. Pilli, Photovoltaic self consumption analysis in a European low voltage feeder, Electr. Power Syst. Res. 194 (June 2020) (2021) 107087, http://dx.doi.org/10.1016/j.epsr.2021.107087.
[77] A. Mangipinto, F. Lombardi, F.D. Sanvito, M. Pavičević, S. Quoilin, E. Colombo, Impact of mass-scale deployment of electric vehicles and benefits of smart charging across all European countries, Appl. Energy 312 (2022) 118676, http://dx.doi.org/10.1016/J.APENERGY.2022.118676.
[78] Electric vehicle conductive charging system - Part 1: General requirements, 2010, IEC61851-1:2010.
[79] S. Cundeva, A.K. Mateska, M.H.J. Bollen, Hosting capacity of LV residential grid for uncoordinated ev charging, in: Proceedings of International Conference on Harmonics and Quality of Power, Vol. 2018-May, ICHQP, IEEE Computer Society, 2018, pp. 1–5, http://dx.doi.org/10.1109/ICHQP.2018.8378892.
[80] J. Sears, D. Roberts, K. Glitman, A comparison of electric vehicle Level 1 and Level 2 charging efficiency, in: 2014 IEEE Conference on Technologies for Sustainability, SusTech 2014, Institute of Electrical and Electronics Engineers Inc., 2014, pp. 255–258, http://dx.doi.org/10.1109/SUSTECH.2014.7046253.
[81] C.D. Cauwer, M. Messagie, S. Heyvaert, T. Coosemans, J.V. Mierlo, Electric Vehicle Use and Energy Consumption Based on Realworld Electric Vehicle Fleet Trip and Charge Data and Its Impact on Existing EV Research Models, World Electr. Veh. J. 2015, Vol. 7, Pages 436-446 7 (3) (2015) 436–446, http://dx.doi.org/10.3390/WEVJ7030436.
[82] Y. Dahmane, R. Chenouard, M. Ghanes, M. Alvarado-Ruiz, Optimized time step for electric vehicle charging optimization considering cost and temperature, Sustain. Energy Grids Netw. 26 (2021) 100468, http://dx.doi.org/10.1016/J.SEGAN.2021.100468.
[83] M. Sameti, F. Haghighat, Integration of distributed energy storage into net-zero energy district systems: Optimum design and operation, Energy 153 (2018) 575–591, http://dx.doi.org/10.1016/J.ENERGY.2018.04.064.
[84] H. Beltran, P. Ayuso, E. Pérez, Lifetime expectancy of Li-ion batteries used for residential solar storage, Energies 13 (3) (2020) 568, http://dx.doi.org/10.3390/en13030568.
[85] R.D. Deshpande, K. Uddin, Physics inspired model for estimating 'cycles to failure' as a function of depth of discharge for lithium ion batteries, J. Energy Storage 33 (2021) 101932, http://dx.doi.org/10.1016/J.EST.2020.101932.
[86] L. Calearo, A. Thingvad, C. Ziras, M. Marinelli, A methodology to model and validate electro-thermal-aging dynamics of electric vehicle battery packs, J. Energy Storage 55 (2022) 105538, http://dx.doi.org/10.1016/J.EST.2022.105538.